Experimental and numerical simulation of wind characteristics behind square prism array windbreaks: Importance of replicating unintended longitudinal turbulence gradients

Junwei Lyu*, Matthew S. Mason and Chien Ming Wang
School of Civil Engineering, The University of Queensland, St Lucia, Queensland 4072, Australia
**Email address: junwei.lyu@uq.net.au*

ABSTRACT

Unintended longitudinal gradients in a short wind tunnel were replicated in numerical simulations by using spires to enable the validation of wake wind speeds behind square prism array windbreaks. Both mean wind speed and turbulence profiles were examined in experiments and simulations where the turbulence model and mesh size were optimized prior to this comparison. A series of simulations without a spire representing the scenario closer to what would exist in reality were also conducted for the comparison study. It was found that in the experiment, the decay of turbulence was significant in the longitudinal direction whereas the mean wind speeds remained nearly unchanged. When the windbreak model was included in simulations, regardless of the spire inclusion, mean wind speeds were well matched with the experimental results. However, the turbulence results could only be reasonably matched when a spire was included in simulations, proving the need of replicating all aspects of an experiment, even if unintended, when undertaking verification simulations.

1. Introduction

Windbreaks are protective obstacles, either vegetative or manmade, for mitigating wind hazards that pose threats to humans and assets. They are gaining more attention in recent years as extreme wind events are intensifying and causing more severe damage to infrastructure and loss of life (Mei & Xie, 2016). To better design windbreaks for more optimal protection, effects of geometric parameters of windbreak arrays on the wind characteristics in the leeward area need to be better understood. A past research study has shown a number of complex geometric characteristics related to the arrangement of windbreaks influencing the sheltering effect they offer (Hong *et al*., 2015). Owing to this complexity, numerical simulations have often been adopted as a study approach as they allow large numbers of cases to be tested once validated (Blocken, 2015).

A present challenge for validating simulations against experiments carried out in short wind tunnels is the unintended, yet unavoidable, longitudinal gradients in these facilities (Lyu *et al*., 2021). These exist because of the wind tunnel size, and the fetch between the turbulence generators (e.g. a spire and a trip board) and the tested model are usually insufficient to allow the boundary layer to be fully developed. As a result, wind speed profiles are often only matched at the incident location, rather than through the entire wake region. As such, variations of both velocity and turbulence profiles after passing the incident location, referred to here as *unintended longitudinal gradients*, can be observed. This creates the need for replicating these gradients in any numerical simulation in order for the validation against experimental results to be valid.

In this paper we seek to show the importance of replicating any unintended longitudinal gradients that may exist within wind tunnel experiments when using them to assess the veracity of numerical simulation outputs. This is done here by comparing wind tunnel measurements in the lee of a single square prism array windbreak configuration with simulation results where longitudinal turbulence gradients are replicated through the introduction of spires and trip boards into the simulation and the alternate case where these are not used. This paper is organized as follows. The wind tunnel experiment and numerical simulation set-up will be presented in Sections 2 and 3. Section 4 will present experimental and numerical results. Section 5 will summarize the key findings.

2. Experimental Set-up

Wind speed measurements in the wake of four different arrangements of square prism arrays with the height H = 0.038m and the width D = 0.022m, as shown in Figure 1, were conducted in the open-circuit suction-type wind tunnel with longitudinal corner fillets in the School of Civil Engineering, The University of Queensland. Each arrangement has a different number of rows or gap between prisms. Owing to space limitation, only one will be shown here. This arrangement is staggered and has a distance of $GapX$ = 2D in the x direction between prisms, a distance of $GapY$ = 4D in the y direction between prims and seven rows in the x direction, as shown in Figure 1.

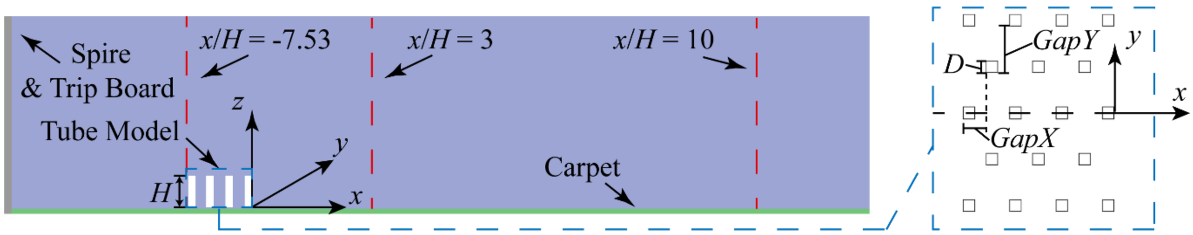

(a) Illustrative figure of experiment set-up

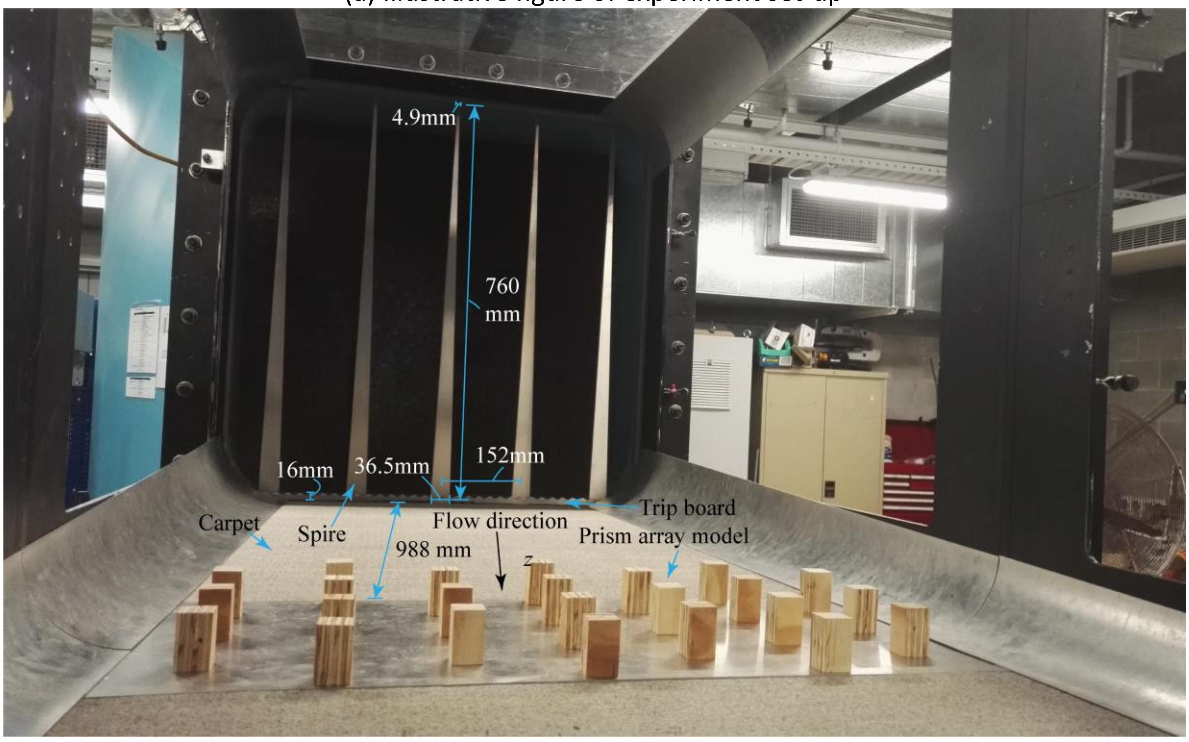

(b) Wind tunnel installation photo

Figure 1. Experiment set-up

A combination of spires, trip boards and carpet, whose dimensions are shown in Figure 1, were chosen after several trials to be installed in the wind tunnel to generate the approach boundary layer wind flow at the scale of 1:100 with the normalized roughness length $z_0/H = 2.63\times10^{-4}$, representing the open sea surface during storms (Wieringa, 1992). The prism array models were installed 26*H* away from the trip board and occupied the entire width of the wind tunnel so that two-dimensional flow condition could be generated. The blockage ratio in the wind tunnel was approximately 5%. A Cobra probe was used to measure velocity profiles at 11 locations ($-7.53 < x/H < 30$) on the centre line of the tunnel ($y/H = 0$), with and without the model present. All the profiles were measured over the depth $0.13 < z/H < 5.26$ with a sampling period of 1 minute and a sampling frequency of 1000 Hz. When the free stream longitudinal mean wind speed $\overline{U}_0 > 14$ m/s, all profile parameters of concern were found to be Reynolds Number independent. Thus $\overline{U}_0 = 14$ m/s was used as the freestream velocity for all tests. Velocity measurements were also conducted at several lateral locations ($-5 < y/H < 5$) at the front of the prism ($x/H = 7.53$, the incident location) in the absence of the prism model to confirm the two-dimensionality of the approach flow.

3. Simulation Set-up

The simulation method, domain size as well as boundary conditions were chosen in accordance with the best practice guidelines summarized by Blocken (2015). All the simulations were conducted with the steady-state double-precision 3D Reynolds-Averaged Navier-Stokes Simulations (RANS) method. As it is shown in Figure 2, the simulation domain has a height of 20*H*, equalling the height of the wind tunnel, a length of 405*H*, ensuring sufficient length for flow development, and a width of 11.6*H*, which was found to be sufficiently wide to have no influence on the results of interests. Zero-static pressure was specified at the domain outlet. Symmetry boundary conditions were imposed on the sides of the domain. The top boundary condition was chosen to be a smooth wall resembling the wind tunnel. The bottom of the domain was simulated to be a wall with the roughness parameter corresponding to the roughness length z_0 used in the experiment.

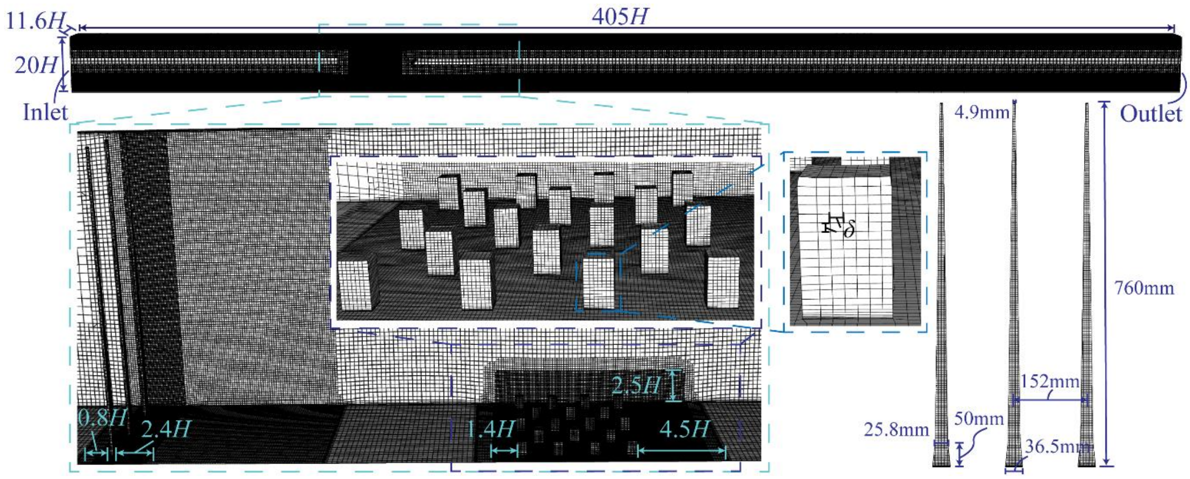

Figure 2. Domain size and meshing for the simulations

Simulations were first run in an identical domain to that shown in Figure 2, but with the prism models removed. These simulations were used to establish the appropriate inlet flow conditions. Two sets of inlet flow conditions were produced. Firstly, in an empty domain without spire or trip board, the objective was to generate longitudinal mean wind speed $\overline{U}$, turbulence kinetic energy *TKE* and specific dissipation rate ω profiles in equilibrium with the domain bottom roughness (matched with z_0 in experiment) without longitudinal gradients. This set of profiles was imposed at the inlet of a domain with the prism model but without a spire or trip board. The second set of profiles, generated in a domain with a spire or trip board, the dimensions of which needed to be trialled, were developed to produce $\overline{U}$ and *TKE* profiles matched with the incident profiles at the model location in the experiment, and to replicate the longitudinal gradients that exist in those tests. The optimal spire or trip board was then built into a domain with the prism model and placed at the same distance away from the model as in the wind tunnel. In this domain with the prism model, a uniform velocity inlet of 20m/s was adopted. After some experimentation it was found that only a spire was needed to match experimental results, with the final dimensions shown in Figure 2. This spire differs marginally from that used in the experiment, because the fillets present in the experiment were not explicitly modelled here.

The cut-cell meshing method was adopted for meshing the domain. This ensures the majority of the grids are hexahedral, with the mesh in the area near the spire and the prism model refined as shown in Figure 2. Outside of this refinement area, the mesh size increases towards the domain boundaries. Ten inflation layers were constructed at the top and bottom boundaries. A mesh sensitivity study was carried out with the minimum meshing size δ varying from 0.003m to 0.01m in five levels to produce results that are not influenced by discretization errors. The final chosen mesh size was δ = 0.00375m.

The SIMPLE algorithm was used for pressure-velocity coupling and hybrid-initialization was applied. Second-order discretization schemes were used for both convection and viscous terms of the governing equations. The Generalized *k-ω* (GEKO) model in ANSYS Fluent was adopted as the turbulence model since it has shown superiority over other commonly-used *k-ε* or *k-w* models after free parameters CMIX and CTurb were tuned (Lyu *et al*., 2021). In this study, CMIX was tuned based on the experimental results of four prism array arrangements from 0.3 (default) to 2, and CTurb was tuned from 0.1 to 2 (default). CMIX = 1, CTurb = 0.1 was found to be the optimal parameter set and adopted for subsequent simulations.

4. Results and discussions

Figure 3 shows the normalized mean wind speed profiles $\overline{U}_{x,z} / \overline{U}_{x,H}$, the turbulence intensity profiles $\sigma_{ux,z} / \overline{U}_{x,z}$ and the normalized turbulence kinetic energy profiles $TKE_{x,z} / \overline{U}_{x,H}^{2}$ measured in the experiment in the absence of the prism model. At the incident location, the profiles at different lateral locations collapse onto each other, confirming the two-dimensionality of the flow. The calculated target mean velocity and turbulence intensity profiles, based on a log-law atmospheric boundary layer with $z_0/H = 2.63\times10^{-4}$, assuming that longitudinal standard deviations are 2.5 times of friction velocity, were well matched. At different longitudinal locations, $\overline{U}_{x,z} / \overline{U}_{x,H}$ profiles show very little difference. However, turbulence profiles $\sigma_{ux,z} / \overline{U}_{x,z}$ and $TKE_{x,z} / \overline{U}_{x,H}^{2}$ show a decreasing trend as *x*/*H* increases. Faster decrease can be observed at higher elevations, suggesting that it is the decay of the bulk turbulence generated by the spire and the trip board that are likely responsible for these undesired longitudinal gradients.

Figure 4 shows the normalized mean wind speed and turbulence kinetic energy profiles simulated in the domains without the prism model. In terms of normalized mean wind speeds, regardless of the spire presence, all profiles at different longitudinal locations match the incident experimental profile well. In terms of the normalized turbulence kinetic energy profiles, the simulation without a spire produced profiles identical at all longitudinal locations and well matched with the incident experimental profile. The simulation with a spire replicated the trend and range of decay observed in the experiment reasonably, but with slightly different magnitudes. At the incident location, the profile is slightly larger at $1<z/H<5$ and smaller at $z/H<1$ than the experiment. At the subsequent longitudinal locations, the magnitude of the profiles are also slightly larger than the experiment.

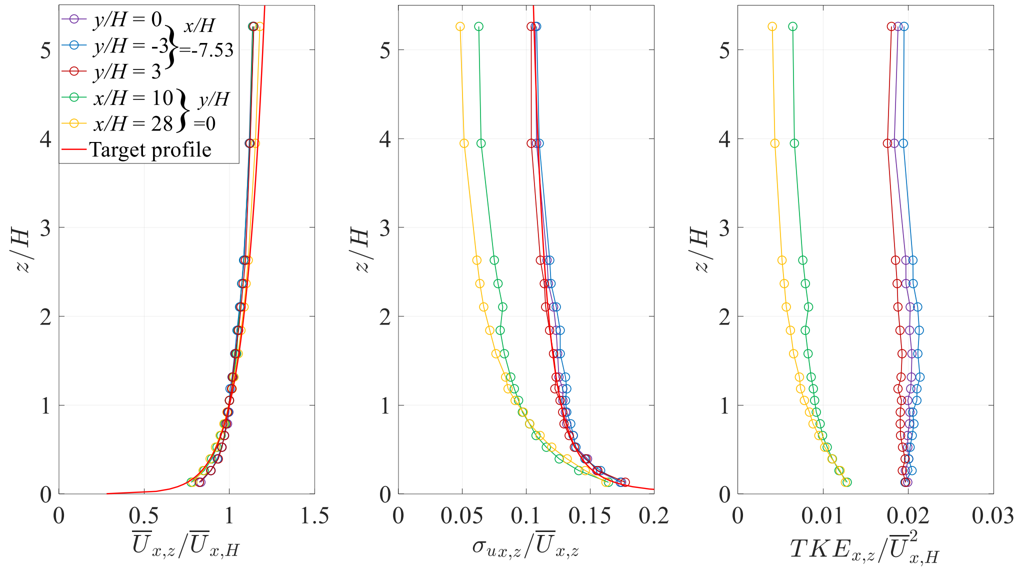

Figure 3. Experimental results in the wind tunnel without the prism model

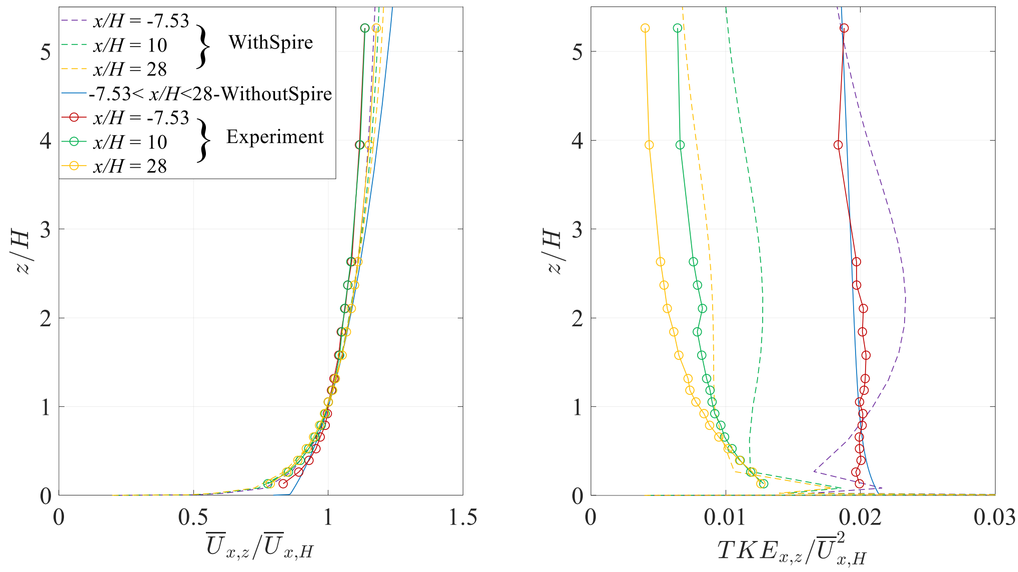

Figure 4. Simulation results in the domains without the prism model

Figure 5 shows the comparison between the experiment and simulations with the prism model. Only the results with the optimal GEKO parameter set are shown here. Local mean wind velocities are normalized by the mean wind velocity at the height *H* and distance *x* in the absence of the prism model with turbulence results shown in the same normalized form and also the normalized deficit form. The deficit form is shown here because of the magnitude difference in the background turbulence when comparing the simulation with a spire and the experiment, as it is shown in Figure 4. It can be seen from Figure 5, all simulations produced mean wind speed results that reasonably match the experimental ones; with the one without the spire producing slightly better results. In terms of turbulence predictions, however, normalized results from the simulation with a spire are much closer to the experimental results than the simulation without a spire. When the background turbulence differences are removed, i.e. in the normalized deficit form, results from the simulation with a spire almost collapse onto the experimental results. This reveals that by only replicating the turbulence decay trend of experiments in simulations with slight differences in magnitude, the turbulence deficit can be well predicted and used to calculate local turbulence magnitudes. However, the elevation of the maximum turbulence in the near lee (e.g. $x/H = 3$) in simulations, indicating the shear layer location, is slightly lower than that in the experiment. The simulation without a spire has consistently higher turbulence than the experiment.

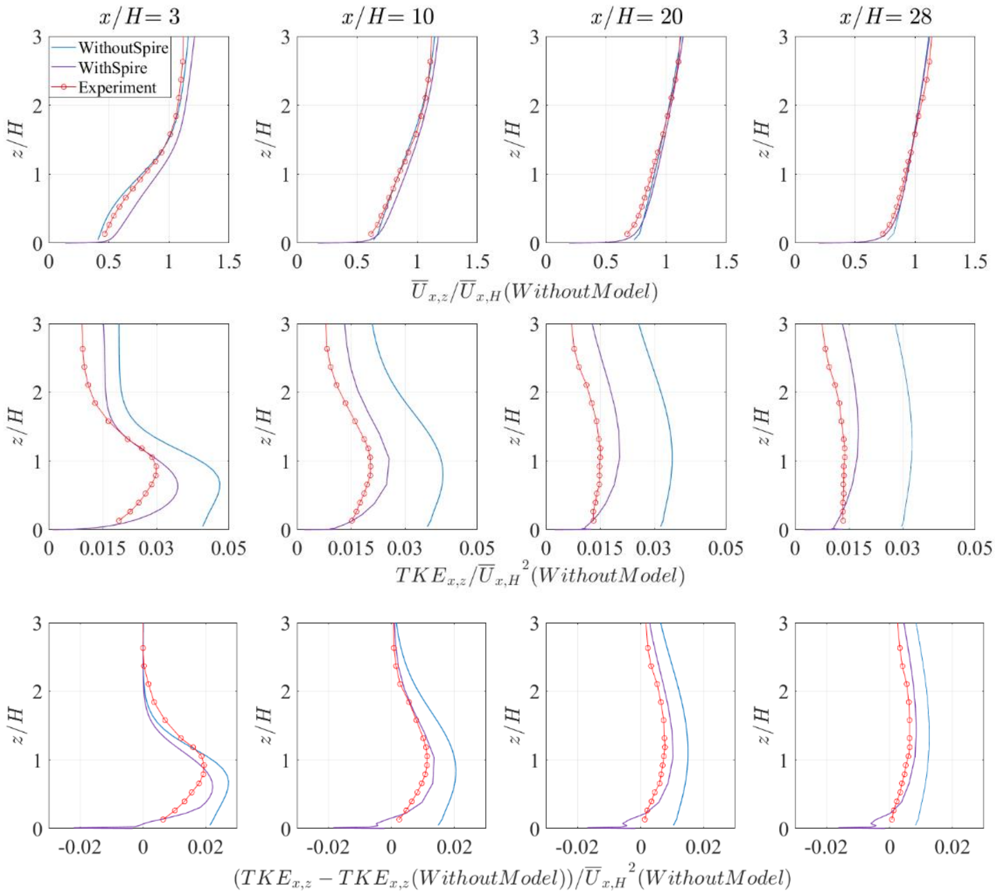

Figure 5. Comparison of simulation and experiment results

5. Conclusions

With the mesh size and the turbulence model optimized, it is found that numerical simulations require the replication of the unintended horizontal turbulence gradients present in wind tunnel experiments in order to replicate those results. This requires a spire to be introduced into the simulation domain in order for the trend and range of simulation results to match those of the experimental results once the prism model is introduced into the domain.

References

Blocken, B. (2015). Computational Fluid Dynamics for urban physics: Importance, scales, possibilities, limitations and ten tips and tricks towards accurate and reliable simulations. *Building and Environment*, 91, 219-245.

Hong, S.-W., Lee, I.-B., and Seo, I.-H. (2015). Modelling and predicting wind velocity patterns for windbreak fence design. *Journal of Wind Engineering and Industrial Aerodynamics*, *142*, 53-64.

Lyu, J., Mason, M. S., and Wang, C. M. (2021). Predicting far-lee wind flow characteristics behind a 2D wedge-shaped obstacle: Experiments, numerical simulations and empirical equations. *Building and Environment*, *194*. https://doi.org/10.1016/j.buildenv.2021.107673

Mei, W., and Xie, S. P. (2016). Intensification of land falling typhoons over the northwest Pacific since the late 1970s. *Nature Geoscience, 9(10), 753-757.*

Wieringa, J. (1992). Updating the Davenport roughness classification. *Journal of Wind Engineering and Industrial Aerodynamics*, *41*(1), 357-368.